ISSN 0016-7029, Geochemistry International, 2016, Vol. 54, No. 7, pp. 569–583. © Pleiades Publishing, Ltd., 2016.
Original Russian Text © A.V. Maslov, V.N. Podkovyrov, G.A. Mizens, A.D. Nozhkin, A.M. Fazliakhmetov, A.I. Malinovsky, A.K. Khudoley, L.N. Kotova, A.V. Kuptsova, E.Z. Gareev, R.I. Zainullin, 2016, published in Geokhimiya, 2016, No. 7, pp. 579–595.

Tectonic Setting Discrimination Diagrams for Terrigenous Rocks: a Comparison

A. V. Maslov[a, b], V. N. Podkovyrov[c], G. A. Mizens[a], A. D. Nozhkin[d], A. M. Fazliakhmetov[b], A. I. Malinovsky [e], A. K. Khudoley[f], L. N. Kotova[c], A. V. Kuptsova[f], E. Z. Gareev[b], and R. I. Zainullin[g, b]

[a] *Institute of Geology and Geochemistry, Ural Branch, Russian Academy of Sciences, ul. Vonsovskogo 15, Yekaterinburg, 620016 Russia*

[b] *Institute of Geology, Ufa Scientific Center, Russian Academy of Sciences, ul. Karla Marksa 16/2, Ufa, 450075 Russia*

[c] *Institute of Precambrian Geology and Geochronology, Russian Academy of Sciences, nab. Makarova 2, St. Petersburg, 199034 Russia*

[d] *Institute of Geology and Mineralogy, Siberian Branch, Russian Academy of Sciences, prosp. Akad. Koptyuga 3, Novosibirsk, 630090 Russia*

[e] *Far East Geological Institute, Far East Branch, Russian Academy of Sciences, prosp. 100 Let Vladivostoku 159, Vladivostok, 690022 Russia*

[f] *St. Petersburg State University, Universitetskaya nab. 7-9, St. Petersburg, 199034 Russia*

[g] *Bashkir State University, ul. Zaki Validi 32, Ufa, 450076 Russia*

e-mail: maslov@igg.uran.ru, mizens@igg.uran.ru, famrb@mail.ru, gareevemir@yandex.ru, vpodk@mail.ru, nozhkin@igm.nsc.ru, malinovsky@fegi.ru, akhudoley@gmail.com, zri-bgu@mail.ru

Received May 6, 2015; accepted May 19, 2015

Abstract—An attempt is made to compare discrimination diagrams of the first (mid-1980s) and second (early 2010s) generations compiled using data for sedimentary successions of different ages. Our results suggest that the diagrams of different generations allow more or less correct discrimination only between the platform, rift, passive margin, and island arc settings. The data for collision sediments do not form separate fields in these diagrams.

Keywords: tectonic discrimination diagrams, rift, island-arc, collision settings, passive margins, Riphean, Phanerozoic

DOI: 10.1134/S0016702916060033

INTRODUCTION

In the last third of the 20th century and early 21st century, whole-rock and trace element geochemistry of sandstones and shales became increasingly used for interpreting paleogeodynamic environments of terrigenous deposition. The first set of diagrams (hereinafter referred to as the first generation diagrams) extensively used in provenance studies was developed in the 1980s on the basis of large geochemical datasets. For example, Maynard et al. (1982) established a discrimination diagram using SiO_2/Al_2O_3 ratio and its covariation with K_2O/Na_2O to classify passive and active continental margin settings. A series of discrimination diagrams, such as $(Fe_2O_3^* + MgO)$–K_2O/Na_2O, $(Fe_2O_3^* + MgO)$–Al_2O_3/SiO_2 and others (Bhatia, 1983) and later SiO_2–K_2O/Na_2O (Roser and Korsch, 1986) were proposed to determine the provenance and tectonic setting of Paleozoic Australian greywackes. All of them are currently used to reconstruct the tectonic setting of sedimentary and metasedimentary rocks of different ages.

The correlations described by Maynard et al. (1982) suggest that the mature terrigenous sediments that were deposited in a passive margin or platform type environment and thus underwent repeated recycling events are characterized by the predominance of K_2O over Na_2O and SiO_2 over Al_2O_3 and occupy the field on the upper right side of the K_2O/Na_2O–SiO_2/Al_2O_3 diagram. In contrast, immature rocks deposited in an active tectonic setting (greywacke and similar rocks) shows relatively low values of the above parameters and plot on the lower left side of the diagram. However, though revolutionary, this diagram does not allow distinction between greywacke and lithic sandstone in island-arc and collision settings. The SiO_2–K_2O/Na_2O plot of Roser and Korsch (1986) works on approximately the same principle. In particular, Bhatia (1983) saw a distinct trend marked by a progressive decrease in TiO_2, $Fe_2O_3^* + MgO$, and

Al_2O_3/SiO_2, and an increase in K_2O/Na_2O and $Al_2O_3/(CaO + Na_2O)$ in sandstone suites from oceanic island arc to continental island arc to active continental margins to passive margins. Except for these diagrams, no new diagrams for tectonic discrimination based on major elements have been proposed during the past 25–30 years while the volume of criticism continues to grow (Armstrong-Altrin and Verma, 2005; Ryan and Williams, 2007; Caracciolo et al., 2012 and others).

We demonstrated in our previous study (Maslov et al., 2012a) using whole-rock geochemistry of Riphean sandstones of the Southern Urals and Kama–Belaya aulacogen and Upper Proterozoic and Phanerozoic silty-sandy rocks of the Russian Plate (Ronov et al., 1995) that the tectonic setting for platform- and subplatform-type psammites can be readily reconstructed using diagrams of Maynard et al. and Roser and Korsch, whereas diagrams of Bhatia are more useful for provenance interpretation of greywacke-type sandstones and forearc sandstones of similar composition.

DF_1–DF_2 DIAGRAMS PROPOSED BY S. VERMA AND J. ARMSTRONG-ALTRIN IN 2013

New discrimination diagrams for terrigenous rocks with high (63–95 wt %) and low (35–63 wt %) $(SiO_2)_{adj}$ contents were published by Verma and Armstrong-Altrin (2013). The field boundaries were obtained from probability calculations as originally proposed by Agrawal (1999) using worldwide examples of Neogene–Quaternary terrigenous sediments from known tectonic settings (island arcs of Kuril–Kamchatka, Japan, Ryuku, Philippines, Tonga, etc.; rifts of Mexico, California, Brazil, Spain, Nigeria, China, Mongolia, etc.; collision zones of Nepal, India, Iran, Italy, Serbia, etc.). For the high-silica diagram with 63 wt % < $(SiO_2)_{adj}$ < 95 wt %, the percent success values for arc, continental rift, and collision settings were about 94–96%, 79–85%, and 83–88%. Similarly, for the diagram with $(SiO_2)_{adj}$ ranging from 35 to 63 wt %, the percent success values for the same settings were ~90%, 75–92%, and 96–100%, which are considerably higher than those of diagrams developed in the 1980s.

These new diagrams (hereinafter referred to as the second generation diagrams) were tested by the authors from two datasets. The first dataset included clastic sediments from known tectonic settings: (1) Miocene–Pleistocene sediment samples from the Shikoku basin (island arc settings); (2) recent sediments of the Baja California (rift settings); (3) recent sands from the Himalayas (collision settings); (4) Pliocene–Pleistocene sediments from the Chile Trench (island arc settings). All of these sediments have percent success of 60% and more.

The second dataset included the results on older sediment samples. For the first application case, the authors used sediments of the Moodies Group of the Barberton greenstone belt (South Africa) deposited in a foreland-type basin (Hessler and Lowe, 2006). The high- and low-silica diagrams showed a collision setting for over 90% of these samples. For the second application case, the authors used shale samples from the Archean Abitibi greenstone belt (Canada). In the high-silica diagram, ~90% of samples were plotted in the arc field, whereas in the low-silica diagram with $(SiO_2)_{adj}$ < 63 wt %, only ~44% of samples did so. However, this result is consistent with the geological observations (Feng and Kerrich, 1990). Another application case included samples of Lower Proterozoic sediments from the Bundelkhand craton (India) deposited in a passive margin setting (Absar et al., 2009). The diagram with $(SiO_2)_{adj}$ > 63 wt % indicated a continental rift setting for about 90% of the sediments of the Gwalior Group, whereas 5 out of 6 samples were plotted in this tectonic field in the low-silica diagram. The last application case in this dataset included Neoproterozoic sediments of the Hammamat Group (Egypt). About 90% of these samples were plotted in the arc field, which seems to be in agreement with the original authors (El-Rahman et al., 2010). At the same time, according to researchers (Holail and Moghazi, 1998; Shalaby et al., 2006), the Hammamat Group is interpreted as molasse-type sediments deposited during the Pan-African orogeny.

COMPARISON OF DISCRIMINATION DIAGRAMS OF DIFFERENT GENERATIONS

In order to compare new diagrams with those developed in the 1980s, we compiled a database[1], which included whole-rock compositions of both sandstone and shale samples from collision, rift, and island arc settings. The *collision settings* are represented either by the so-called unfolded molasses, such as Upper Vendian sandstones from the Belomor–Kuloy plateau, northwestern Mezen' syneclise, Dnestr pericraton, and Shkapovo–Shikhan depression (Sochava et al., 1992; Sokur, 2012) or by molasse sediments, such as sandstones from the Olyutor terrane (Aluga and Pakhacha Formations) and Kamchatka (Malinovsky, 1986, 1993; Geosynclinal..., 1987); sandstones of the uppermost Asha Group, Southern Urals (Bekker, 1988); shales of the Shuntara, Potoskuy and other Riphean formations of the Yenisei Ridge (Nozhkin et al., 2013; Likhanov et al., 2014); sandstones of the Upper Permian-Lower Triassic molasse sequence of the Ural Foredeep (Mizens, 1997; Tverdokhlebov, 2001). The *rift settings* are represented by sandstones of the Priozernaya and Salmin Formations of the Early Riphean Pasha–Ladoga graben (Amantov and Spiridonov, 1989; Kheraskova et al., 2006; Kuptsova et al., 2011); sandstones and

[1] The analytical data used in this study will be available from the first author to interested persons upon request via e-mail.

shales of the Riphean Ai and Mashak Formations, Southern Urals (Formation..., 1986; Parnachev et al., 1986); sandstones of the Riphean Prikamsk Formation of the Kama–Belaya aulacogen (Lozin, 1994; Belokon' et al., 2001); terrigenous sediments of the Kar'ernaya, Lopatin and other formations of the Riphean Chingasan Group, Yenisei Ridge (Nozhkin et al., 2007, 2008), and terrigenous sediments of the Riphean Uya Group, Uchur–Maya region (Khudoley et al., 2001; Podkovyrov et al., 2002). The *arc settings* are represented by tephra deposits (Maslov et al., 1984), sandstones[2] of the Ryskuzhino, Ulutau and other Devonian formations of the Western Magnitogorsk zone, Southern Urals (Yazeva and Bochkarev, 1998; Mizens, 2002); Paleoproterozoic metasedimentary and metamorphic rocks of the Kan block at the southern folded margin of the Siberian platform (Nozhkin et al., 2001; Dmitrieva et al., 2008); Upper Riphean metasedimentary rocks of the Arzybei terrane of the Sayan–Yenisei accretionary–collisional belt (Rumyantsev, 2001; Dmitrieva et al., 2006), and Upper Riphean metasedimentary rocks of the Yudino and Predivinsk sequences within the Predivinsk terrane from the same region (Chernykh, 2000; Nozhkin et al., 2013).

In order to test the diagrams, we also used whole-rock data set for terrigenous rocks deposited in *platform* and *passive continental margin settings*. These included the platform deposits of the Athabasca Group, Canada (Semikhatov, 1974; Rainbird et al., 2007; Jefferson et al., 2007); Lower and Middle Riphean shales of the Southern Urals (Parnachev, 1995; Maslov et al., 2012a); sandstones and shales of the Trekhgornaya and other Riphean formations of the Uchur–Maya region (Podkovyrov et al., 2002; Maslov et al., 2012b); silty–sandy rocks of the Shaim petroleum region, West Siberia (Fedorov et al., 2009); Vendian argillaceous–silty rocks of the Nepa–Botuoba anteclise (Shemin, 2007; Fomin et al., 2013). The *passive continental margin settings* are represented by terrigenous rocks of the Karatau Group, Southern Urals (Maslov et al., 2002) and metapelites of the Uderei, Gorbilok, and Korda Formations of the Yenisei Ridge (Nozhkin et al., 2008; Vernikovsky et al., 2009).

Locations of these samples (except the Athabasca Group) are shown in Fig. 1. Samples were selected to cover a wide range of possible ages and geographic regions and to extend the database to include known tectonic settings, which have been overlooked in some way by S. Verma and J. Armstrong-Altrin. Our database comprises whole-rock compositions of 720 sandstone samples and over 300 shale samples. Major elements in bulk samples of these rocks were analyzed in different years by classical wet chemistry and XRF at central integrated laboratory facilities of Bashkirgeologiya, Sevzapgeologiya, Uralgeologiya, Department of Natural Resources of the Ural Federal District, Institute of Geology of the Bashkir Branch of the USSR Academy of Sciences, Institute of Geology of the Ufa Scientific Center of the Russian Academy of Sciences, Institute of Geology and Geochemistry of the Ural Branch, Russian Academy of Sciences, All-

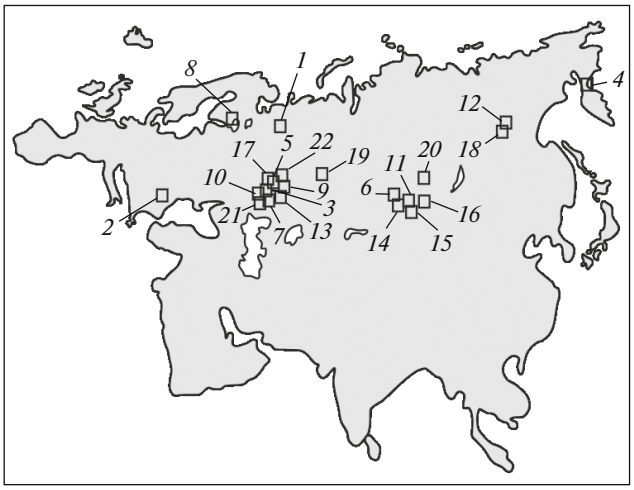

Fig. 1. Locations of sediment samples of different ages and geodynamic settings, whose whole-rock compositions were used in this study. *1–7*—sediments from collision settings (*1*—Upper Vendian sandstones from the northwestern part of the Mezen' depression, *2*—sandstone of the same age from the Dnestr pericraton, *3*—Upper Vendian sandstones from the Shkapovo–Shikhan depression, *4*—sandstones from the volcanic molasse of the Olyutor terrane, *5*—sandstones from the uppermost part of the Vendian Asha Group of the Southern Urals, *6*—shales of the Shuntara, Potoskuy, Sosnovka and other Riphean formations of the Yenisei Ridge, *7*—sandstones from the Late Permian–Lower Triassic molasse of the Belaya depression, Ural Foredeep; *8–12*—rift-related sediments (*8*—sandstones from the Priozernaya and Salmin Formations of the Pasha–Ladoga graben, *9*—sandstones and shales from the Ai and Mashak Formations of the Southern Urals, *10*—sandstones from the Prikamsk Formation of the Kama–Belaya aulacogen, *11*—terrigenous sediments from the Kar'ernaya, Lopatin and other formations of the Chingasan Group, Yenisei Ridge, *12*—terrigenous rocks of the Uy Group, Uchur–Maya region); *13–16*—island arc rocks (*13*—dominantly tuffaceous sandstones of the Ryskuzhino, Ulutau and other Devonian formations of the Western Magnitogorsk zone, *14*—Paleoproterozoic metasedimentary rocks of the Arzybei block, southern folded margin of the Siberian platform, *15*—Riphean metasedimentary rocks of the Kan terrane, *16*—metamorphic rocks of the Yudino and Predivinsk sequences of the Predivinsk terrane, Sayan–Yenisei accretionary–collisional belt); *17–20*—platform sediments (*17*—Lower and Middle Riphean shales of the Southern Urals, *18*—sandstones from different lithostratigraphic units of the Riphean hypostratotype and Trekhgornaya Formation shales of the Uchur–Maya region, *19*—Jurassic silty–sandy rocks of the Shaim and other petroleum regions of West Siberia, *20*—Upper Vendian clayey-silty rocks of the Nepa–Botuoba anteclise); *21, 22*—passive margin rocks (*21*—shales and sandstones of the Karatau Group, Southern Urals, *22*—shales of the Uderei, Gorbilok, and Korda Formations of the Yenisei Ridge).

[2] Clastic material that forms part of these sedimentary successions has experienced no reworking because it was transported just after eruption and deposited by turbidity currents to deep-water depressions adjacent to island arcs (Maleev, 1980).

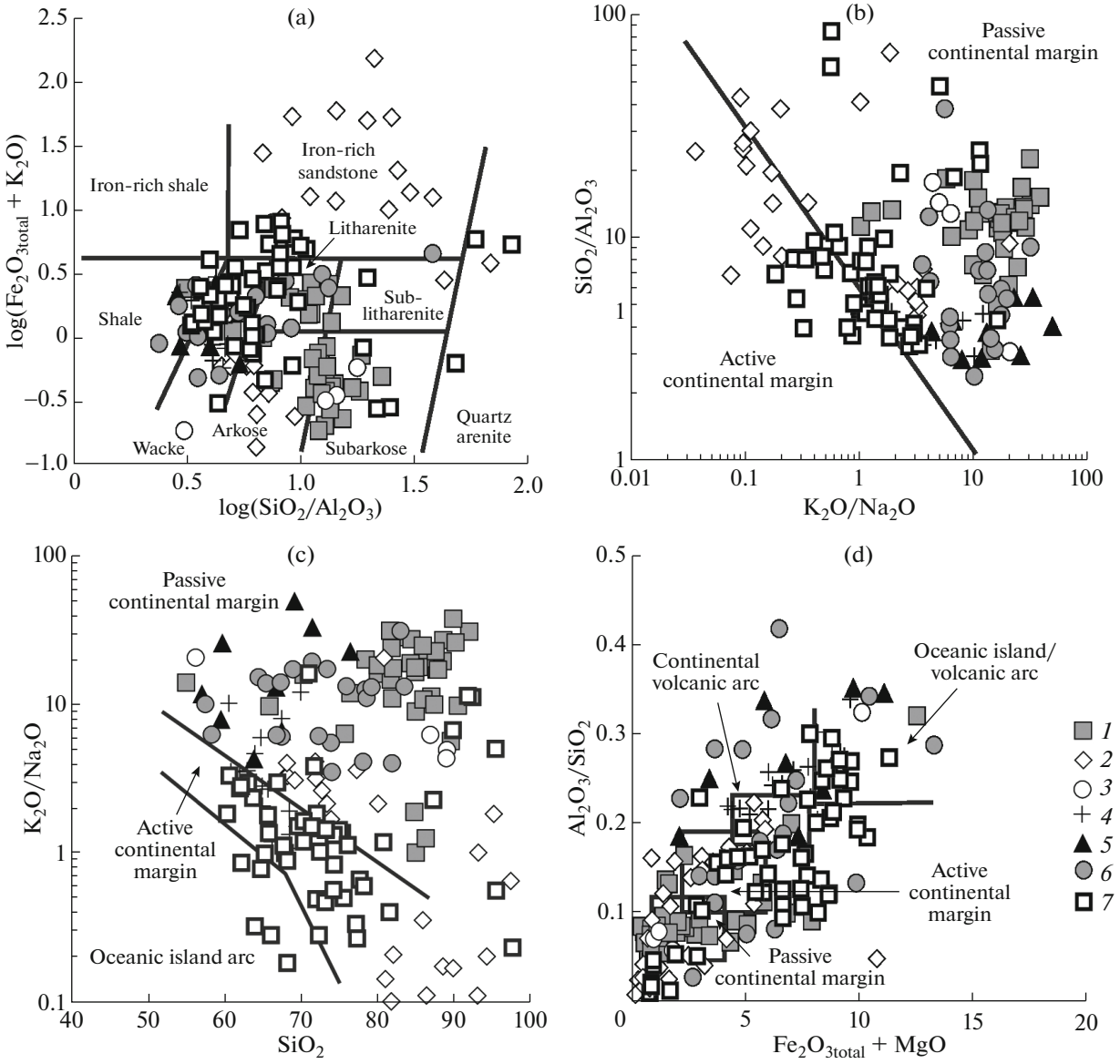

Fig. 2. Distribution of data for terrigenous rocks from rift settings in the diagrams of Herron (a), Maynard et al. (b), Roser and Korsch (c), and Bhatia (d). *1*—Riphean sandstones of the Pasha–Ladoga graben; *2*—sandstones of the Aya and Mashak Formations, Southern Urals; *3*—sandstones of the Kama Formation of the Kama–Belaya aulacogen; *4*—shales of the Aya and Mashak Formations; *5*—terrigenous rocks from the Kar'ernaya, Lopatin and Olen'in Formations, Yenisei Ridge; *6*—terrigenous rocks of the Chingasan Group from the same structural unit; *7*—sandstones and shales of the Uy Group, Uchur–Maya region.

Russia Research Institute of Geology (VSEGEI), Ural State Mining University, Institute of Geology and Mineralogy of the Siberian Branch, Russian Academy of Sciences, Institute of the Earth's Crust of the Siberian Branch, Russian Academy of Sciences, and Far East Geological Institute of the Far east Branch, Russian Academy of Sciences.

FIRST GENERATION DIAGRAMS

In the $\log(SiO_2/Al_2O_3)$–$\log(Fe_2O_3^*/K_2O)$ diagram of Herron (1988), the studied sandstone and shale rocks deposited in *rift settings* occupy the fields for shale, wacke, litharenite, and arkose (Fig. 2a). Some of the samples can be classified as sub-arkose. In the K_2O/Na_2O–SiO_2/Al_2O_3 diagram (Maynard et al., 1982), the majority of the terrigenous sediment samples lie close to the field of the passive continental margin setting (Fig. 2b). A different pattern is observed when some sandstones from the Aya and Mashak Formations of the Southern Urals and the Uy Group from the Uchur–Maya region plot in the field of passive continental margins, with few tending toward the field of active continental margins.

In the SiO_2–K_2O/Na_2O diagram (Roser and Korsch, 1986), all of the clastic sedimentary rocks

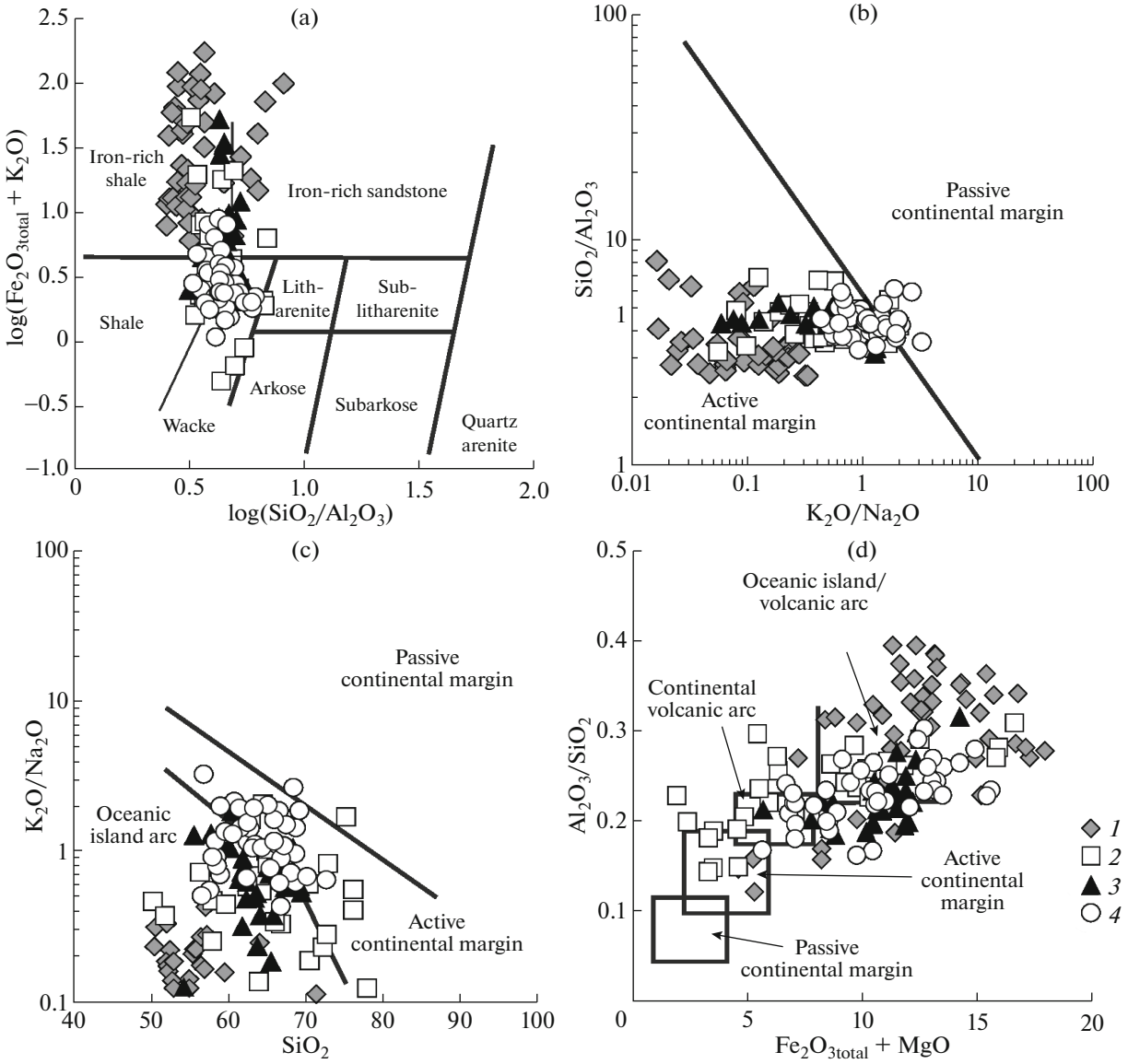

Fig. 3. Distribution of data for terrigenous rocks from island arc settings in the diagrams of Herron (a), Maynard et al. (b), Roser and Korsch (c), and Bhatia (d). *1*—Devonian tuffaceous sandstones from the Western Magnitogorsk zone, Southern Urals; *2*—metaterrigenous rocks of the Yudino and Predivinsk sequences of the Predivinsk terrane; *3*—metaterrigenous rocks of the Arzybei terrane; *4*—metaterrigenous rocks of the Kan block.

from rift settings exhibit a broadly similar pattern, although there are slight differences (Fig. 2c). For example, the majority of the Uy Group terrigenous samples from the Uchur–Maya region plot in the field of active continental margins, with few in the island arc field. The majority of the Ai and Mashak shale samples fall within the passive margin field, although few plot in the island arc field. Sandstones from the Priozernaya and Salmi Formations of the Pasha–Ladoga graben tend to have the highest SiO_2 and K_2O/Na_2O contents.

A slightly different situation is observed for sandstones and shale samples of rift settings in the ($Fe_2O_3^*$ + MgO)–Al_2O_3/SiO_2 diagram (Bhatia, 1983): the majority of the Pasha–Ladoga graben sandstone samples tend to form a tight cluster around the passive margin field (Fig. 2d). In the diagram of Herron, the majority of psammites and shales originally deposited in *an island arc setting* plot in the fields for shale, wacke, iron-bearing shale and sandstone (Fig. 3a). The exception is the Devonian psammites from the Western Magnitogorsk zone of the Southern Urals, which fall in the fields of iron-bearing shale and sandstone.

In the K_2O/Na_2O–SiO_2/Al_2O_3 diagram, almost all our samples from the samples of known island arc settings plot within the field of active continental margins

(Fig. 3b). Only 7 out of 42 samples of high-K migmatized garnet-biotite gneisses of the Kan block plot outside this field. In the SiO_2–K_2O/Na_2O diagram, almost all samples of island arc settings fall outside the field of passive continental margins (Fig. 3c). Here, the field of active continental margins is defined by most of the Kan block samples, which are regarded as deposited in the active continental margin/ensialic arc settings (Nozhkin et al., 2001), and almost half of feldspar quartzites from the Predivinsk and Yudino sequences. The remaining samples fall within the field of the active island arc setting.

In the $(Fe_2O_3^* + MgO)$–Al_2O_3/SiO_2 diagram, ~ 8% of the samples from the island arc setting falls within the field of active continental margins (Fig. 3d). The remaining samples plot within the continental and oceanic arc fields, with the latter field being defined mostly by Middle Devonian psammites from the paleo-island arc segment of the Southern Urals.

The database for terrigenous rock samples of known *collision settings* mostly includes sandstones plotting as wacke, litharenite, and arkose in the diagram of Herron (most of the psammite samples from the Upper Vendian molasse of the Southern Urals plot as litharenite and wacke, with only a few trending toward sub-litharenite) (Fig. 4a). Shales of the Shuntara, Potoskuy, Sosnovka, and Pogoryui Formations of the Yenisei Ridge plot as shale and wacke.

In the K_2O/Na_2O–SiO_2/Al_2O_3 diagram, the sandstones and shales plot mostly in the passive continental margin field (Fig. 4b). A few psammite samples from the Upper Vendian successions of the Southern Urals and Belomor–Kuloy plateau plot in the field of active continental margins. Most of the Upper Vendian sandstones in the unfolded molasse of the Shkapovo–Shikhan depression fall within the same field. All sandstone samples from volcanic molasse sequences of the Olyutor terrane plot in the active continental margin field.

In the SiO_2–K_2O/Na_2O diagram, the distribution of psammites from volcanic molasse sequences is somewhat curious, because almost all of them fall within the oceanic island arc field (Fig. 4c). The other psammites from the Upper Vendian molasse of the Southern Urals and unfolded molasse of the Shkapovo–Shikhan depression plot in the active continental margin field. At the same time, the psammites from the Upper Vendian unfolded molasse of the Belomor–Kuloy plateau and Dnestr pericraton, as well as shales from the Shuntara, Sosnovka and other formations of the Yenisei Ridge were deposited in the collision setting (Likhanov et al., 2014 and others).

In the $(Fe_2O_3^* + MgO)$–Al_2O_3/SiO_2 diagram, the majority of sandstones in the unfolded molasse of the Belomor-Kuloy plateau, Dnestr pericraton, and Shkapovo–Shikhan depression (Fig. 4d), as well as the psammites in the Upper Devonian molasse of the Southern Urals trend toward the passive and active continental margin fields. The sandstones in the volcanic molasse of the Olyutor terrane fall within the fields of active continental margins and continental island arcs. The Upper Riphean shales of the Yenisei Ridge with high Al_2O_3/SiO_2 and Fe_2O_3 + MgO trend toward the oceanic arc field.

The distribution of our samples from the *platform setting* in the diagram of Herron clearly indicates their assignment to a wide range of psammites and iron-rich shales (Fig. 5a). The average composition of Phanerozoic cratonic sandstones (PrCS)[3] (Condie, 1993) in this diagram plots in the sub-litharenite field, whereas that of post-Archean Australian shales (PAAS) (Condie, 1993) plot in the shale field.

In the K_2O/Na_2O–SiO_2/Al_2O_3 diagram, nearly all of the studied sandstones and shales classified as platform or similar type deposits on the basis of geological criteria cluster within the passive continental margin field (Fig. 5b). The average data of PAAS plot in the same field. The only exception appears to be Jurassic samples from the western part of West Siberia, which plot mostly in the active continental margin field. In the SiO_2–K_2O/Na_2O diagram (Fig. 5c), their compositions fall within the active continental margin and oceanic island arc fields. Assuming there were no analytical errors, the above sediments should be composed mostly of the material reworked into the West Siberian basin from destroyed island arc associations of the Urals. The remaining sandstones and shales in our database that were deposited in platform settings plot in the passive margin field similar to the average compositions of model sandstones and PAAS.

In the $(Fe_2O_3^* + MgO)$–Al_2O_3/SiO_2 diagram, the passive margin field, which should supposedly comprise all our terrigenous samples from the platform settings, contains only about 60–70% of Riphean sandstones from the Uchur–Maya region, a portion of Jurassic silty psammites from the West Siberian basin, and Athabasca sandstones (Fig. 5d). The great majority of these sandstones, similar to shales of the Riphean Bakal, Zigazy–Komarovo, and Avzyan Formations of the Southern Ural trend toward the continental and oceanic volcanic arc fields, whereas the Jurassic psammites fall mostly within the active margin and continental volcanic arc fields. The latter two fields as well as the oceanic arc field comprise the majority of the Vendian shales from the Nepa–Botuoba anteclise. The average composition of silty–sandy sediments from the Russian plate falls in the active margin field, whereas while the average compositions of PrCS and PAAS plot in the passive margin and oceanic volcanic arc fields, respectively. These results support our previous conclusion (Maslov et al., 2012a) that the diagrams of Bhatia cannot be correctly

[3] Compositions of silty-sandy rocks of the Russian plate and PrCS are considered hereinafter as the model compositions.

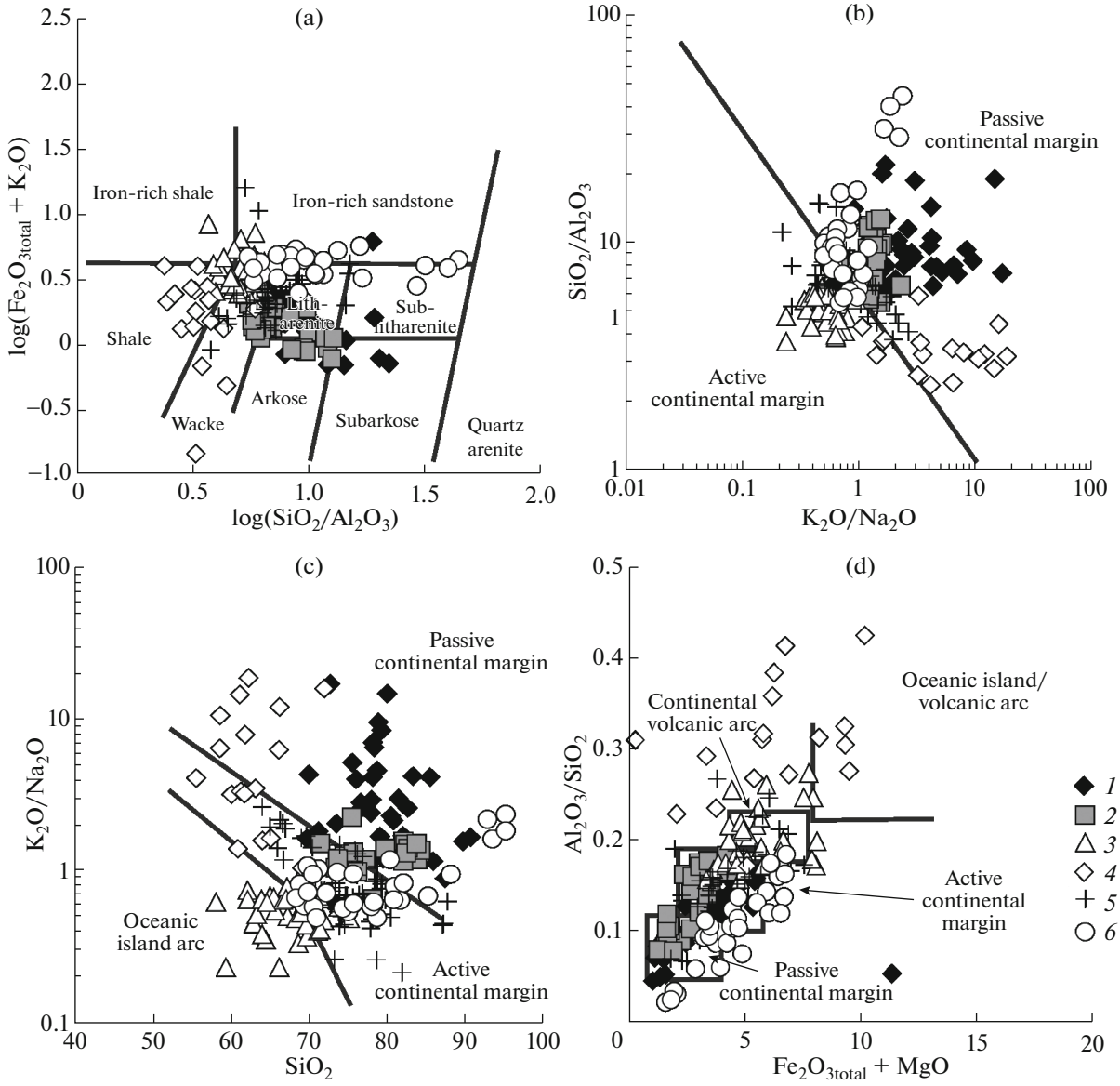

Fig. 4. Distribution of data for terrigenous rocks from collision settings in the diagrams of Herron (a), Maynard et al. (b), Roser and Korsch (c), and Bhatia (d). *1*—Upper Vendian sandstones of the Belomor–Kuloy plateau; *2*—Upper Vendian sandstones of the Dnestr pericraton; *3*—sandstones of the Aluga and Pakhacha Formations, Olyutor terrane; *4*—shales of the Shuntara, Potoskuy, Sosnovka Formations, Yenisei Ridge; *5*—Upper Vendian sandstones of the Shkapovo–Shikhan depression; *6*—Upper Vendian sandstones of the Bashkir megaanticlinorium.

used for discriminating platform setting sediments, although they contain the field for terrigenous samples from passive margin settings, i.e., in other words, the least active tectonic settings).

Shale samples from the Karatau Group of the South Urals, as well as from the Uderei, Gorbilok, and Korda Formations of the Yenisei Ridge, which were deposited in an environment similar to the *passive margin setting*, plot within the wacke and shale fields in the diagram of Herron (Fig. 6a). The Karatau Group sandstones are classified as litharenites, sub-litharenites, arkoses, subarkoses, and quartz arenites. This compositional heterogeneity should govern to some extent the distribution of sediment types in different discrimination diagrams. However, this is not always true.

In the K_2O/Na_2O–SiO_2/Al_2O_3 diagram, nearly all sandstone and shale samples from the above two localities plot in the passive continental margin field and differ only in their SiO_2/Al_2O_3 content (Fig. 6b). These results are consistent with the geological observations. In the SiO_2–K_2O/Na_2O diagram, shales of the Uderei, Gorbilok, and Korda Formations of the Yenisei Ridge form a tight cluster in the active margin

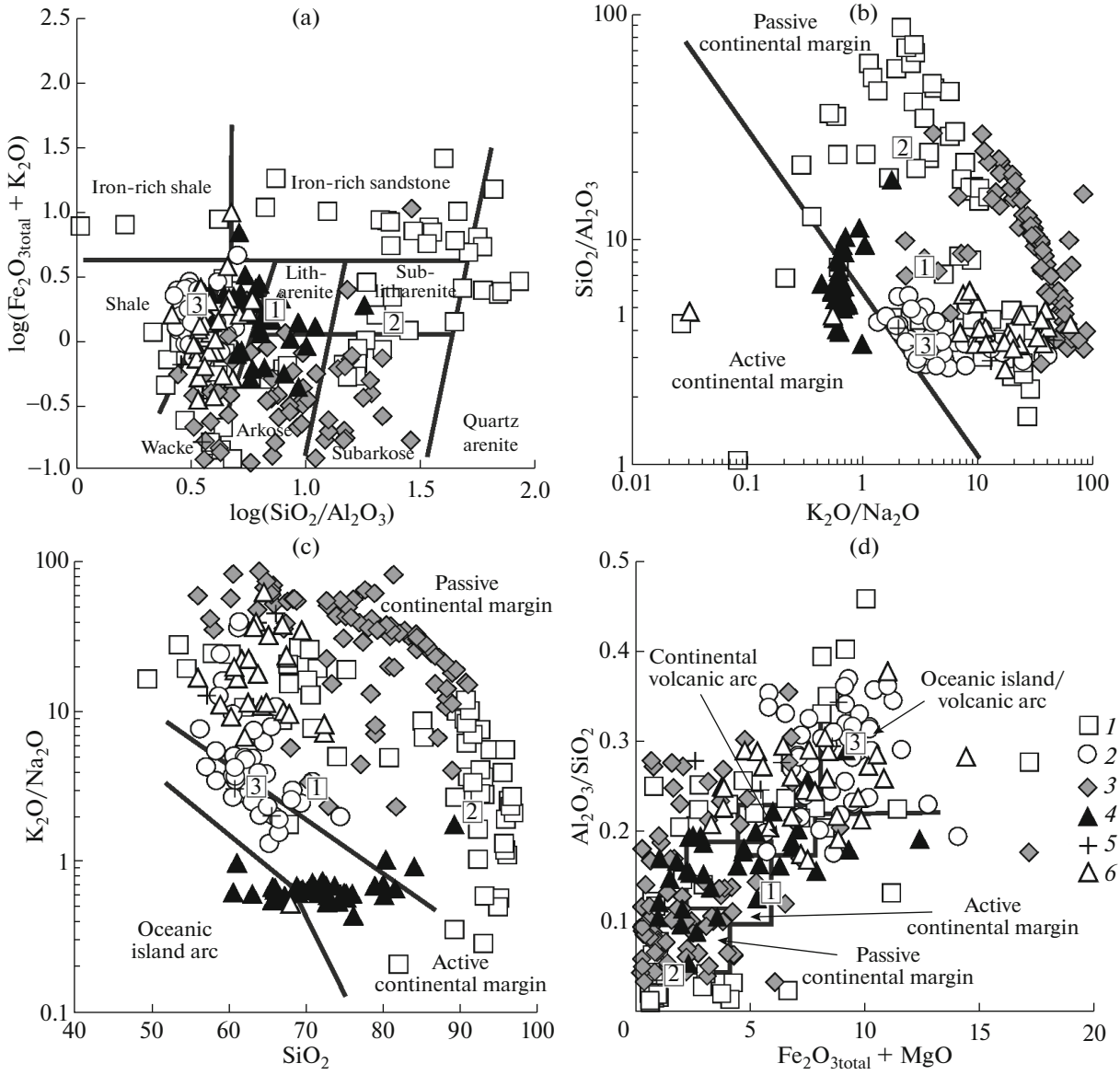

Fig. 5. Distribution of data for terrigenous rocks from platform and similar type settings in the diagrams of Herron (a), Maynard et al. (b), Roser and Korsch (c), and Bhatia (d). *1*—Athabasca sandstones; *2*—Lower–Middle Riphean shales of the Bashkir megaanticlinorium; *3*—sandstones of the Dim, Omakhta, Gonam, and Trekhgornaya Fms. of the Uchur–Maya region; *4*—sandstones and silty sandstones of the Shaim and other petroleum regions of West Siberia; *5*—Trekhgornaya Fm. shales of the Uchur–Maya region; *6*—Upper Vendian shales of the Nepa–Botuoba anteclise. Numbers in squares: 1—silty–sandy rocks of the Russian plate (Ronov and Migdisov, 1996); 2—PrCS (Condie, 1993); 3—PAAS (Condie, 1993).

field (Fig. 6c). Sandstones and shales of the Karatau Group, though trending toward the field for passive continental margins, show a wider scatter, which is indicative of a wide variation in their deposition environments. Of particular interest is the distribution of sandstones and shales from the passive margin setting in the $(Fe_2O_3^* + MgO)$–Al_2O_3/SiO_2 diagram (Fig. 6d), in which ~80–85% of the Karatau Group sandstones plot in the passive continental margin field, whereas the associated shales mostly fall in the field of continental and oceanic island arcs. The shales of the Uderei, Gorbilok, and Korda Formations of the Yenisei Ridge show a broadly similar pattern. These results illustrate clearly the well-known assumption that sandstones are more reliable indicators of the tectonic setting than shales (Taylor and McLennan, 1988).

In all three diagrams, the Karatau Group sandstones generally fall within the passive continental margin field. At the same time, shales samples exhibit more variable patterns: they trend toward the passive margin field in the diagram of Maynard et al., mostly cluster in the active continental margin field in the

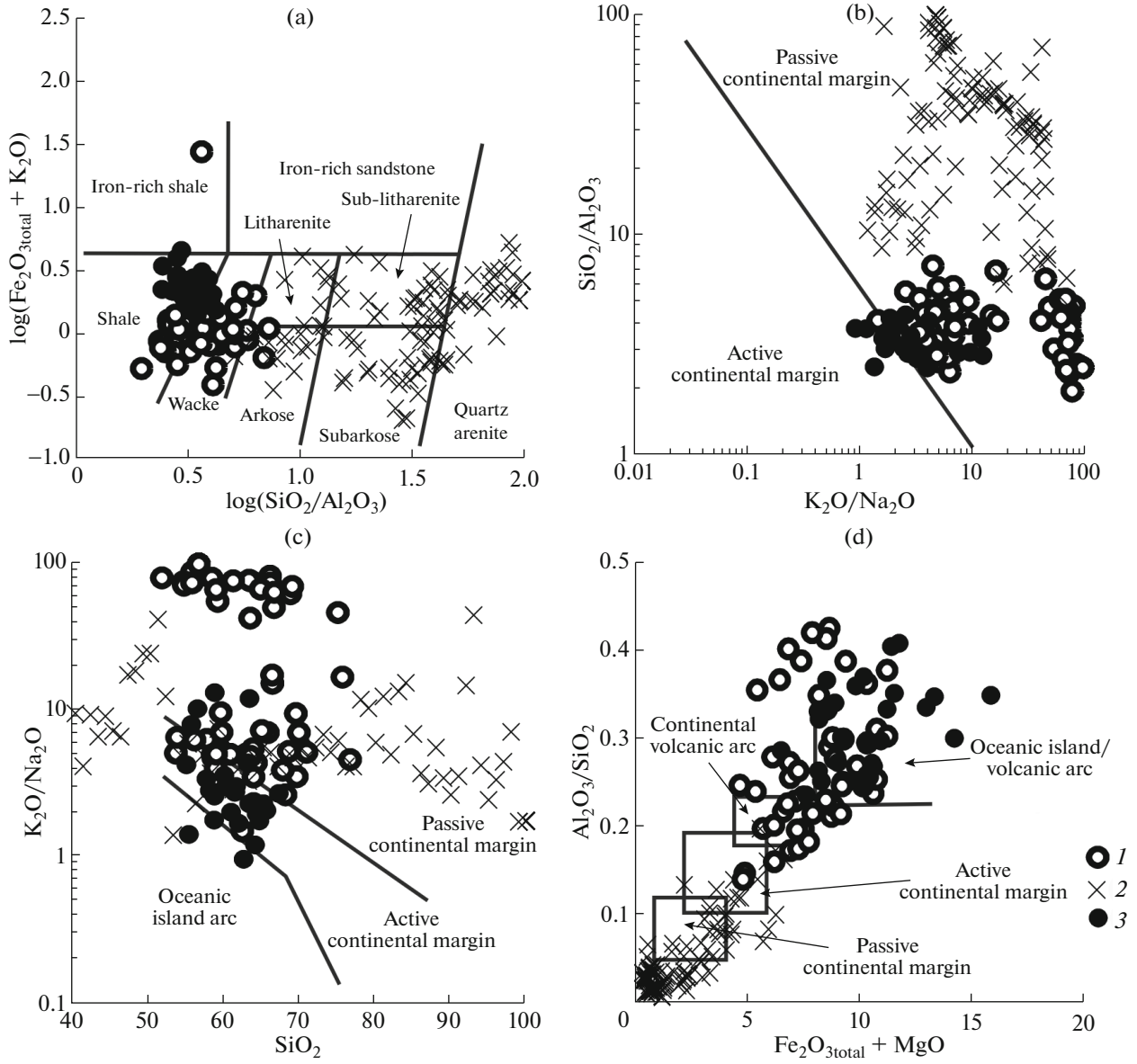

Fig. 6. Distribution of data for terrigenous rocks from passive continental margin settings in the diagrams of Herron (a), Maynard et al. (b), Roser and Korsch (c), and Bhatia (d). *1*—Karatau Group shales of the Bashkir megaanticlinorium; *2*—Karatau Group sandstones; *3*—Uderei, Gorbilok, and Korda Fms. shales of the Yenisei Ridge.

diagram of Roser and Korsch, or fall within the island arc fields in the diagram of Bhatia.

SECOND GENERATION DIAGRAMS

Because the great majority of sandstones and shales from the *rift settings* or similar settings are characterized by $(SiO_2)_{adj} > 63\%$, we used the high-silica diagram (Fig. 7a). If we abstract from the fields defined by specific samples in this diagram, it can be clearly seen that nearly two thirds of all samples correspond to a compositional field representing, according to S. Verma and J. Armstrong-Altrin, the rift settings, and one third of samples are collision sediments. A similar pattern is observed for each locality in our database, except the Uy Group. About 80% of the samples from this group plot in the rift setting, while the remaining samples fall mostly in the collision setting.

We used both diagrams of S. Verma and J. Armstrong-Altrin for discriminating terrigenous sediment samples from our database that were deposited in the *island arc setting*, because all of them represent both the high-silica and low-silica types. The diagram with $(SiO_2)_{adj} > 63\%$ confirmed this setting only for the Middle Devonian sandstones from the eastern slope of the Southern Urals. Metasedimentary rocks from the

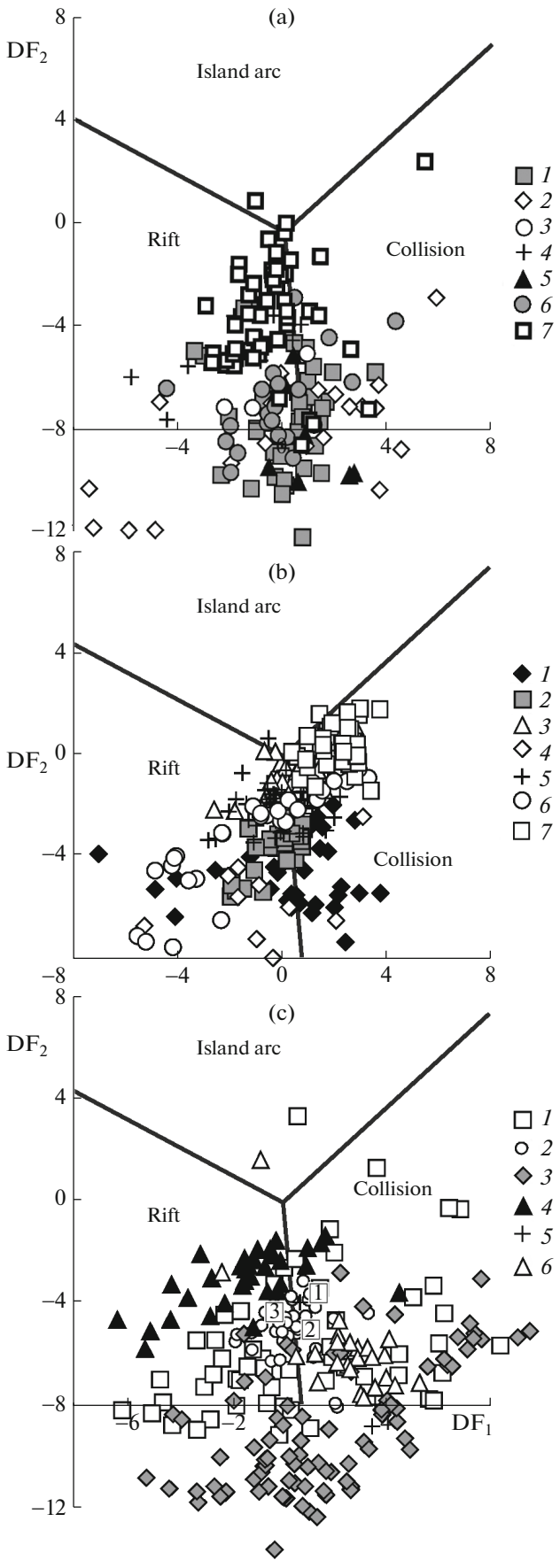

Predivinsk terrane and Kan block clustered in nearly equal proportions into the rift and collision settings while the samples from the Arzybei terrane mostly fell within the collision setting (Fig. 8a). In the diagram with $(SiO_2)_{adj} < 63\%$, ~100% of the Devonian sandstone samples of the Southern Urals (Fig. 8b) plot in the island arc setting, which is consistent with the geology of this region. The same field also comprises a great number of samples from the Yudino and Predivinsk sequences of the Predivinsk and Arzybei terranes, whereas metasedimentary rocks from the Kan block mostly trend toward the rift and collision settings or plot slightly toward the field boundaries. The interpretation of the results has to bear in mind that the metasedimentary sequence of the Predivinsk terrane composed of a series of tectonic slices also contains volcanics, which were formed both in island arc and rift (backarc) settings, and that some high-silica samples from our database, such as mica-feldspar quartzites and some schists, may represent rift settings. The above-mentioned scatter in the diagram DF_1–DF_2 is probably related to amphibolite-facies metamorphism in the Kan block.

The great majority of our samples from the *collision settings* belong to the high-silica type. The respective diagram confirmed this setting for ~80–85% of the sandstones from the Ural Foredeep molasse (Fig. 7b). The remaining samples were distributed between the rift and collision settings, with the number of samples plotting in the rift setting being often somewhat higher. The Upper Vendian molasse sandstones of the Southern Urals tended to plot in the rift setting, which is inconsistent with the inference of some authors (Bekker, 1988; Puchkov, 2000 and others), but is in agreement with other authors (Rusin, 1998).

In order to analyze the distribution patterns of sandstone and shale samples from the *platform settings* in the second generation diagrams, we added a number of platform-type sediment samples and samples from other rock associations in the diagram with $(SiO_2)_{adj} > 63\%$, because these compositions were absent from this diagram. As a result, the samples formed two clusters in the rift and collision fields (Fig. 7c), while most of the Riphean sandstones from the Uchur–Maya region plotted outside the field defined by values $-8 < DF_2 < +8$.

DISCUSSION AND CONCLUSIONS

The distribution of sandstone and shale samples in discrimination diagrams of the first and second gener-

Fig. 7. Distribution of data for terrigenous rocks from rift (a), collision (b), and platform (c) settings in the high-silica DF_1–DF_2 diagram. a: for symbols, see Fig. 2. b: *7*—Upper Permian–Lower Triassic sandstones of the Belaya depression, Ural Foredeep. The remaining symbols are the same as in Fig. 4. c: for symbols, see Fig. 5.

ations shows that the terrigenous sediment samples from the rift or similar settings mostly plot within the passive continental margin field in the diagrams of Maynard et al. and Roser and Korsch. A few samples tend toward the active margin field, indicating that almost all sediments from the above tectonic fields were deposited in a relatively calm tectonic regime.

In the $(Fe_2O_3^* + MgO)–Al_2O_3/SiO_2$ diagram, the rift sediments from in our database show more or less uniform distribution between the four expected tectonic fields. These results indicate that this diagram cannot be used for discriminating the provenance of such sediments, because it was compiled using the chemical compositions of rocks from continental arc settings.

The terrigenous samples from the collision settings show a slightly different distribution pattern in the first generation diagrams. For example, from 2/3 to 3/4 of all samples plot in the passive margin field in the diagram of Maynard et al. More than half of the samples from this setting plot in the active margin field in the diagram of Roser and Korsch, while in the $(Fe_2O_{3tot} + MgO)–Al_2O_3/SiO_2$ diagram, they are distributed between the passive continental margin, active continental margin, and continental arc fields, which does not allow us to come to any certain conclusion.

Our previous analysis of lithogeochemical characteristics of fine-grained clastic sedimentary rocks from the Vendian folded and unfolded molasse of the Southern and Middle Urals, eastern and northeastern parts of the Russian platform (Maslov et al., 2013b) shows that these samples are distributed between the passive margin, active margin, and oceanic island arc fields in the $SiO_2–K_2O/Na_2O$ diagram. They form an array oriented nearly perpendicular to the field boundaries. These results suggest the absence of any significant homogenization for the psammite (Maslov et al., 2013a) and shale compositions in tectonically active collision settings. Whole-rock compositions of shales reflects characteristics of rock associations formed at different evolutionary stages of orogenic belts, because of the presence of tectonic blocks of different lithologies and tectonic settings in the source areas.

In addition, our results are consistent with the conclusion that some commonly used discrimination diagrams (mostly $K_2O/Na_2O–SiO_2/Al_2O_3$ and $SiO_2–K_2O/Na_2O$) work more or less effectively for the discrimination of tectonic settings for platform sedimentary successions. The diagrams of Bhatia, which were originally compiled for terrigenous rock from island and continental arc settings, do not work properly for most of the analyzed sediments.

The distributions of our terrigenous samples in the diagram of Maynard et al. show no principal differences between platform, rift, and passive margin sediments. The only thing that is worth noting is a slight, as yet theoretical possibility of subdividing this diagram into three discrimination fields (Fig. 9a): 1) terrigenous sediments from relatively active tectonic settings; 2) sediments from passive continental margin, collision, and rift (?) settings; 3) platform sediments. The latter representing repeatedly recycles provenances are characterized by the highest values of both K_2O/Na_2O and SiO_2/Al_2O_3 (Athabasca sandstones or Lower-Middle Riphean psammites of the Uchur–

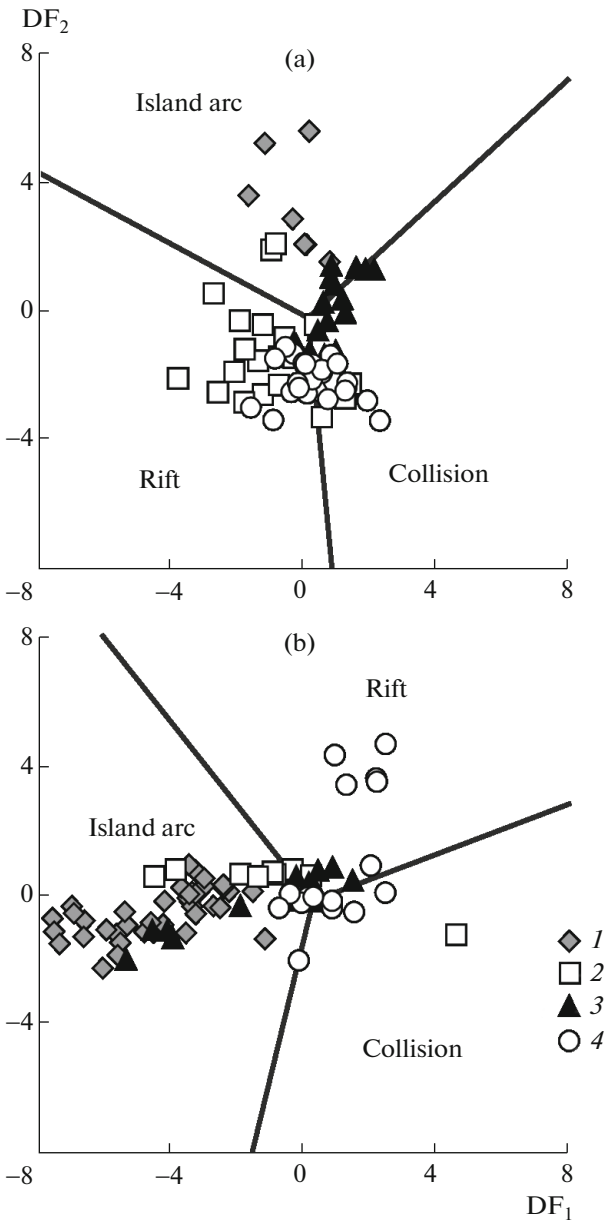

Fig. 8. Distribution of data for terrigenous rocks from island arc settings in thehigh-silica (a) and low-silica (b) $DF_1–DF_2$ diagrams. *1*—Devonian tuffaceous sandstones from the Western Magnitogorsk zone, Southern Urals; *2*—metaterrigenous rocks of the Yudino and Predivinsk sequences of the Predivinsk terrane; *3*—metaterrigenous rocks of the Arzybei terrane; *4*—metaterrigenous rocks of the Kan block.

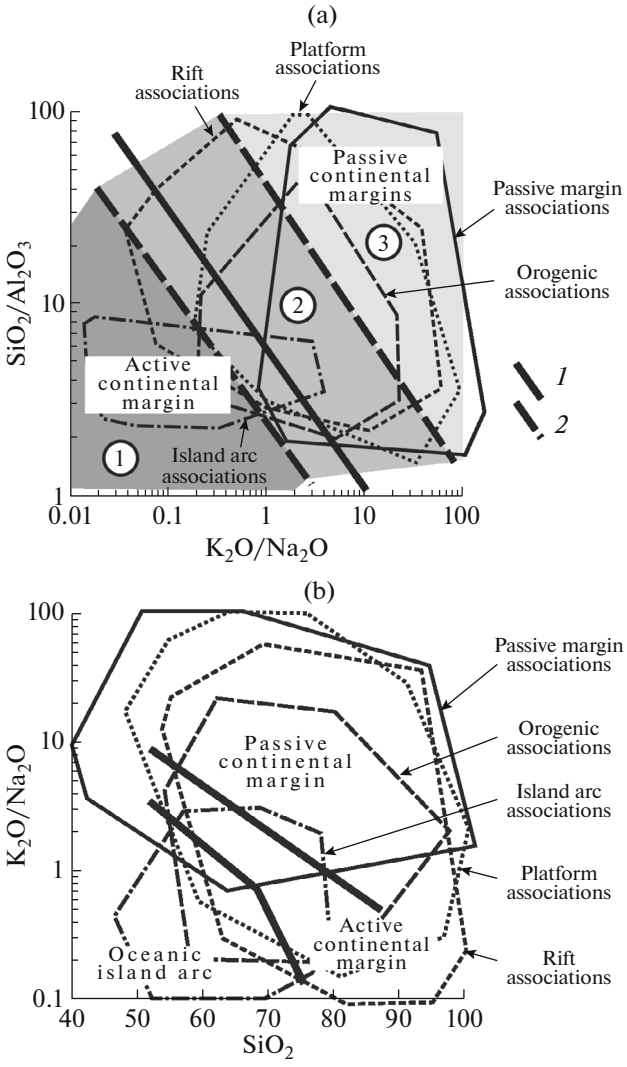

Fig. 9. Location of fields defined by terrigenous rocks from different geodynamic settings in the diagrams of Maynard et al. (a) Roser and Korsch (b). *1*—boundary between the active margin and passive margin rocks; *2*—inferred boundaries between terrigenous rocks from different continental margins and platform (intracratonic) areas (see text for explanation).

Maya region). Their K_2O/Na_2O values reflect the well-known tendency of alkalis in sedimentary processes, i.e., the preferential mobilization of potassium into the weathering crusts and platform deposits and removal of sodium into the ocean. The rocks representing island arc associations have lower K_2O/Na_2O and SiO_2/Al_2O_3 and differ considerably from terrigenous sediments from other tectonic settings. The rocks from the collision-related settings can be found both in the passive margin and active continental margin fields (Fig. 9a).

In the diagram of Roser and Korsch, the terrigenous sediments from platform, passive margin, rift, and collision associations appear to have too much overlap (more than 60–70%) for any definable separation between the individual provenances. The field of island arc associations trends toward the lower values of SiO_2 and K_2O/Na_2O, but it also has a ~50% overlap with the above-mentioned fields (Fig. 9b).

The high-silica DF_1–DF_2 diagram (Fig. 10) shows subtle differences between the common fields of sandstones and shales from platform, rift, and collision settings. The only visible difference is that the minimum DF_2 values of collision sediments are not higher than –8, whereas many rift-related compositions in our database are characterized by $-13 < DF_2 < -8$. In addition, this diagram shows no arrays that can be attributed to a single discrimination field. They usually overlap into rift and collision provenances. The island arc compositions are shifted toward the values of $-4 < DF_2 < +6$, at relatively constant DF_1 values (–5, –4...+4). At the same time, the island arc psammites from the Western Magnitogorsk zone of the Southern Urals plot within the respective field consistent with their geological situations in both high-silica and low-silica diagrams, whereas metasedimentary rocks from various structural elements of the Yenisei Ridge and its margins tend to plot toward the field boundaries. Therefore, this diagram does in discriminating their provenances, despite the close location of these sediments to their source areas. It can thus assumed that, unlike the predominantly tuffaceous psammites of the Southern Urals, the metasedimentary rocks from the Predivinsk and Arzybei terranes as well as the Kan block of the Yenisei Ridge are composed of volcano–terrigenous material, the bulk chemical composition of which has undergone transformation before burial in continental or shallow-water environments. Therefore, the diagrams belonging to both generations allow more or less correct discrimination only between the platform, rift, passive margin, and island arc settings. The data for collision sediments do not form separate fields in these diagrams.

The selection of reference geological objects can play a substantial, if not decisive, role in the compilation of tectonic discrimination diagrams. For example, the second generation diagrams have relied on data from continental rifts of California, Brazil, Spain, Nigeria, Uganda, Zambia, Australia, China, Mongolia, etc. At the same time, the bulk compositions of sediments from the East African rift zone (the dominance of different magmatic rock associations in the source areas) should be a priori different from those of the rocks comprising the Rhine graben (the dominance of sedimentary rocks in the source areas), Baikal rift or Viking graben. We think that yet another substantial difficulty with the compilation of the universal discrimination diagram will arise due to the fact that the evolution of many orogenic belts cannot be accounted for by a single event, but by multiple events that have operated on difference scales (Maslov et al., 2015 and references therein), such as collisions of var-

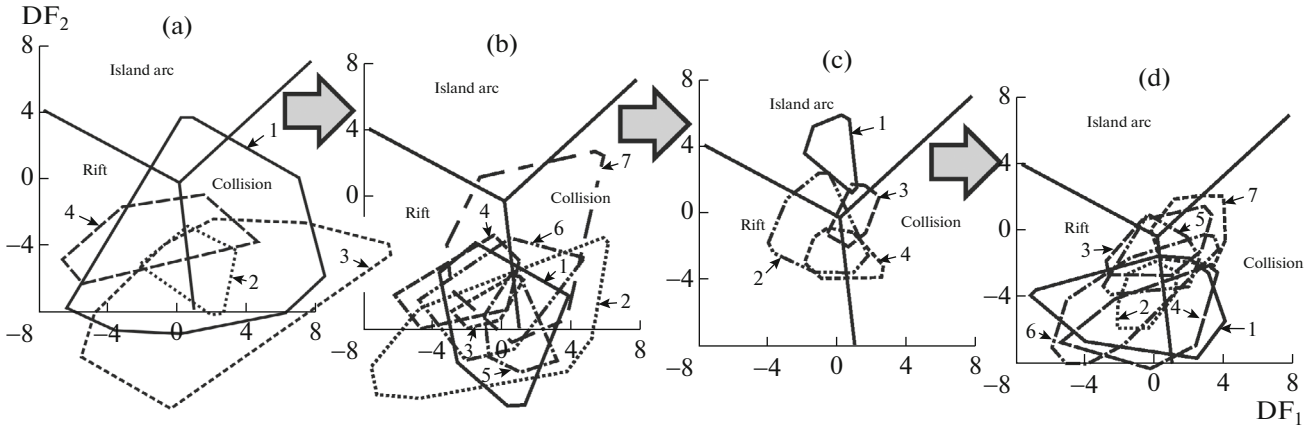

Fig. 10. Location of fields defined by terrigenous rocks from platform (a), rift (b), island arc (c), and collision (d) settings in the high-silica DF_1–DF_2 diagram. The field numbers are the same as in Figs. 7 and 8.

ious zones, blocks, segments, and orogens and hypercollision that continued during much of the geodynamic cycle in which the orogen was formed. In particular, block collision in the Southern Urals occurred in the Lower–Middle Devonian and was related to the collision of blocks that are now incorporated into the composite Mugodzhary terrane, while the collision of orogens took place in the Late Carboniferous (Necheukhin and Volchek, 2012). It is not clear for us how all these variations can be accounted for by a single discrimination diagram, but the research in this direction should be continued.

REFERENCES

N. Absar, M. Raza, M. Roy, S. M. Naqvi, and A. K. Roy, "Composition and weathering conditions of Paleoproterozoic upper crust of Bundelkhand craton, Central India: records from geochemistry of clastic sediments of 1.9 Ga Gwalior Group," Precambrian Res. **168**, 313–329 (2009).

S. Agrawal, M. Guevara, and S. P. Verma, "Tectonic discrimination of basic and ultrabasic rocks through log-transformed ratios of immobile trace elements," *Int. Geol. Rev*. **50**, 1057–1079 (2008).

A. V. Amantov and M. A. Spiridonov, "Geology of Lake Ladoga," Sov. Geologiya, No. **4**, 83–86 (1989).

J. S. Armstrong-Altrin and S. P. Verma, "Critical evaluation of six tectonic setting discrimination diagrams using geochemical data of Neogene sediments from known tectonic settings," Sediment. Geol. **177**, 115–129 (2005).

Yu. R. Bekker, *Precambrian Molasses* (Leningrad, Nedra, 1988) [in Russian].

T. V. Belokon, V. I. Gorbachev, and M. M. Balashov, *Structure and Ore Potential of the Riphean–Vendian Deposits of the Eastern Russian Platform* (IPK Zvezda, Perm', 2001) [in Ryussian].

M. R. Bhatia, "Plate tectonics and geochemical composition of sandstones," J. Geol. **91**, 611–627 (1983).

L. Caracciolo, H. von Eynatten, R. Tolosana-Delgado, S. Critelli, P. Manetti, and P. Marchev, "Petrological, geochemical, and statistical analysis of Eocene–Oligocene sandstones of the Western Thrace basin, Greece and Bulgaria," J. Sediment. Res. **82**, 482–498 (2012).

A. I. Chernykh, Extended Abstract of Candidate's Dissertation in Geology and Mineralogy (OIGGGM, Novosibirsk, 2000) [in Russian].

K. C. Condie, "Chemical composition and evolution of the upper continental crust: contrasting results from surface samples and shales," Chem. Geol. **104**, 1–37 (1993).

N. V. Dmitrieva, O. M. Turkina, and A. D. Nozhkin, "Petrogeochemical features of metaterrigenous rocks of the Kan Block of the eastern Sayan: reconstructions of provenances and sedimentation conditions," Lithol. Miner. Resour. **43** (2), 165–179 (2008).

N. V. Dmitrieva, O. M. Turkina, and A. D. Nozhkin, "Geochemical features of metaterrigenous rocks of the Arzybei and Derba Blocks of the Neoproterozoic accretionary belt of the southwestern framing of the Siberian craton: reconstruction of provenances and sedimentation conditions," Litosfera, No. **3**, 28–44 (2006).

Yu. N. Fedorov, A. V. Maslov, V. P. Alekseev, M. Yu. Fedorov, and Yu. L. Ronkin *Geochemical features of the Tyumen Formation in some areas of West Siberia, in Ways of Implementation of Petroleum and Ore Potential of the Khanty Mansi Autonomous District of Yugra* (Khanty-Mansiisk, 2009), Vol. 1, pp. 182–190.

R. Feng and R. Kerrich, "Geochemistry of fine-grained clastic sediments in the Archean Abitibi greenstone belt, Canada: implications for provenance and tectonic setting," Geochim. Cosmochim. Acta. **54**, 1061–1081 (1990).

A. M. Fomin, M. V. Lebedev, and S. A. Moiseev, "Proposal for refinement of the Vendian stratigraphic scheme of northeastern Nepa–Botuoba anteclise," in Interexpo GEO–Siberia–2013 (SGGA, Novosibirsk, 2013), pp. 29–33 [in Russian].

Formation of the Earth's Crust of the Urals, Ed. by S. N. Ivanov (Nauka, Moscow, 1986) [in Russian].

Geosynclinal Lithogenesis on the Continent–Ocean Boundary (Nauka, Moscow, 1987) [in Russian].

M. M. Herron, "Geochemical classification of terrigenous sands and shales from core or log data," J. Sediment. Petrol. **58**, 820–829 (1988).

A. M. Hessler and D. R. Lowe, "Weathering and sediment generation in the Archean: an integrated study of the evolution of siliciclastic sedimentary rocks of the 3.2 Ga Moodies Group, Barberton Greenstone Belt, South Africa," Precambrian Res. **151**, 185–210 (2006).

H. M. Holail and A.-K. M. Moghazi, "Provenance, tectonic setting and geochemistry of greywackes and siltstones of the Late Precambrian Hammamat Group, Egypt," Sediment. Geol. **116**, 227–250 (1998).

C. W. Jefferson, D. J. Thomas, S. S. Gandhi, P. Ramaekers, G. Delaney, D. Brisbin, C. Cutts, D. Quirt, P. Portella, and R. A. Olson "Unconformity-associated uranium deposits of the Athabasca Basin, Saskatchewan and Alberta," in *EXTECH IV: Geology And Uranium Exploration Technology Of The Proterozoic Athabasca Basin, Saskatchewan And Alberta*, Geol. Surv. Can. Bull. **588**, 23–67 (2007).

T. N. Kheraskova, Yu. A. Volozh, N. G. Zamozhnyaya, S. A. Kaplan, and A. K. Suleimanov, "Structure and history of the western East European Platform in the Riphean–Paleozoic: EV-1 geotraverse data (Lodeinoe Pole–Voronezh)," Litosfera, No. **2**, 65–94 (2006).

V. V. Khomentovsky, "Upper Riphean of the Yenisei Ridge," Russ. Geol. Geophys. **48** (9), 711–720 (2007).

A. K. Khudoley, R. H. Rainbird, R. A. Stern, A. P. Kropachev, L. M. Heaman, A. M. Zanin, V. N. Podkovyrov, V. N. Belova, and V. I. Sukhorukov "Sedimentary evolution of the Riphean–Vendian Basin of southeastern Siberia," Precambrian Res. **111**, 129–163 (2001).

I. V. Khvorova and M. N. Il'inskaya "Comparative characteristics of two volcanosedimentary formations of the South Urals," in *Volcanosedimentary and Terrigenous Formations* (AN SSSR, Moscow, 1963), pp. 87–160 [in Russian].

A. V. Kuptsova, A. K. Khudoley, W. Davis, R. H. Rainbird, V. P. Kovach, and N. Yu. Zagornaya, "Age and provenances of sandstones from the Riphean Priozersk and Salmi formations in the eastern Pasha–Ladoga Basin (southern margin of the Baltic Shield)," Stratigr. Geol. Correlation **19** (2), 125–140 (2011).

I. I. Likhanov, A. D. Nozhkin, V. V. Reverdatto, and P. S. Kozlov "Grenville tectonic events and evolution of the Yenisei Ridge at the western margin of the Siberian craton," Geotectonics **48** (5), 3701–389 (2014).

E. V. Lozin, *Tectonics and Oil Potential of the Platform Bashkortostan* (VNIIOENG, Moscow, 1994), Vol. 1 [in Russian].

E. F. Maleev, *Volcanic Rocks: A Reference Book* (Nedra, Moscow, 1980) [in Russian].

A. I. Malinovsky, "Molasse sandstones of the Olyutorsky trough of East Kamchatka as indicator of tectonic setting of sedimentation," in *Geosynclinal Volcanosedimentary Formations of Far East,* (DVNTs, Vladivostok, 1986), pp. 68–89 [in Russian].

A. I. Malinovsky, *Cenozoic Molasse of the Southern Koyrak Highland* (Dal'nauka, Vladivostok, 1993) [in Russian].

V. A. Maslov, O. V. Artyushkova, and V. N. Baryshev, *Stratigraphy of the Ore-Bearing Devonian Deposits of the Sibai Region* (BFAN SSSR, Ufa, 1984) [in Russian].

A. V. Maslov, G. A. Mizens, V. N. Podkovyrov, A. D. Nozhkin, T. M. Sokur, A. I. Malinovsky, A. A. Sorokin, Yu. N. Smirnova, E. Z. Gareev, N. V. Dmitrieva, M. T. Krupenin, and E. F. Letnikova, "Synorogenic Clay rocks: specifics of bulk composition and paleotectonics," Geochem. Int. **53** (6), 510–533 (2015).

A. V. Maslov, G. A. Mizens, V. N. Podkovyrov, E. Z. Gareev, A. A. Sorokin, Yu. N. Smirnova, and T. M. Sokur, "Synorogenic psammites: major lithochemical features," *Lithol. Miner. Resour.* ***48*** (1), 74–98 (2013a).

A. V. Maslov, E. Z. Gareev, and M. V. Isherskaya, "Standard "discriminant" paleogeodynamic diagrams and platrfom sandstone associations," *Otechestvennaya Geol.* (3), 55–65 (2012a).

A. V. Maslov, V. G. Olovyanishnikov, and M. V. Isherskaya, "Riphean of the eastern, northeastern, and northern periphery of the Russian Platform and western megazone of the Urals: lithostratigraphy, conditions of formation, and types of sedimentary sequences," Litosfera, No. **2**, 54–95 (2002).

A. V. Maslov, V. N. Podkovyrov, and E. Z. Gareev, "Evolution of the paleogeodynamic settings of the formation of the Lower and Middle Riphean sedimentary sequences of the Uchur–Maya region and the Bashkir meganticlinorium," Russ. J. Pac. Geol. **31** (5), 382–394 (2012b).

A. V. Maslov, V. N. Podkovyrov, D. V. Grazhdankin, Yu. N. Fedorov, and E. Z. Gareev, "Some lithogeochemical features of the fine-grained clastic rocks of the folded and non-folded Vendian molasse (western megazone of the South and Middle Urals, east and northeast Russian Platform)," Litosfera (1), 17–35 (2013b).

J. B. Maynard, R. Valloni, and Ho Shing Ju, "Composition of modern deep-sea sands from arc-related basin," J. Geol. Soc. Am. Spec. Publs., No. 10, 551–561 (1982).

G. A. Mizens, "On the stages of formation of the Uralian Foredeep," Geotectonics **31** (5), 33-46 (1997).

G. A. Mizens, *Late Devonian–Early Permian Sedimentation Basins and Geodynamic Settings in the South Urals* (IGG UrO RAN, Yekaterinburg, 2002) [in Russian].

V. M. Necheukhin, and E. N. Volchek, "Types of accretionary and collisional processes in the orogenic systems of the Timan–Ural segment of Eurasia," Litosfera, No. **4**, 78–90 (2012).

A. D. Nozhkin, A. A. Postnikov, K. E. Nagovitsin, A. V. Travin, A. M. Stanevich, and D. S. Yudin, "Neoproterozoic Chingasan Group in the Yenisei Ridge: new data on age and deposition environments," Russ. Geol. Geophys. **48** (12), 1015–1025 (2007).

A. D. Nozhkin, N. V. Dmitrieva, P. A. Serov, and A. V. Maslov, "Petrogeochemical and isotope peculiarities of supersubduction terrigenous deposits: the example of Predivinsk Terrane of the Yenisei Ridge," Dokl. Earth Sci. **452** (2), 1039–1041 (2013).

A. D. Nozhkin, O. M. Turkina, E. V. Bibikova, and V. A. Ponomarchuk, "Structure, composition, and formation conditions of metasedimentary–volcanogenic

complexes of the Kan greenstone belt (northwestern Sayan region)," Russ. Geol. Geophys. **42** (7), 1058–1078 (2001).

A. D. Nozhkin, O. M. Turkina, T. B. Bayanova, N. G. Berezhnaya, A. N. Larionov, A. A. Postnikov, A. V. Travin, and R. E. Ernst "Neoproterozoic rift and within-plate magmatism in the Yenisei Ridge: implications for the breakup of Rodinia," Russ. Geol. Geophys. **49** (7), 503–518 (2008).

A. D. Nozhkin, L. K. Kachevskii, and N.V. Dmitrieva, "The Late Neoproterozoic rift-related metarhyolite–basalt association of the Glushikha rought (Yenisei Ridge): geochemical composition, age, and formation conditions," Russ. Geol. Geophys. **54** (1), 44–54 (2013).

V. P. Parnachev, "Depression–rift setting of the Ripheides of the western slope of the South Urals, in *General Problems of the Riphean Stratigraphy and Geological History of Northern Eurasia* (IGG UrO RAN, Yekaterinburg, 1995), pp. 77–78.

V. P. Parnachev, A. F. Rotar', and Z. M. Rotar', *Middle Riphean Volcanosedimentary Association of the Bashkirian Megantyclinorium (South Urals)* (UNTs AN SSSR, Sverdlovsk, 1986) [in Russian].

V. N. Podkovyrov, V. P. Kovach, and L. N. Kotova, "Mudrocks from the Siberian Hypostratotype of the Riphean and Vendian: chemistry, Sm–Nd isotope systematics of sources, and formation stages," Lithol. Miner. Resour. **37** (4), 397–418 (2002).

V. N. Puchkov, *Paleogeodynamics of the South and Midde Urals* (Dauriya, Ufa, 2000) [in Russian].

R. H. Rainbird, R. A. Stern, N. Rayner, and C. W. Jefferson, "Age, provenance and regional correlation of the Athabasca Group, Saskatchewan and Alberta, constrained by igneous and detrial zircon geochronology," *EXTECH IV: Geology And Uranium Exploration Technology of the Proterozoic Athabasca Basin, Saskatchewan and Alberta*. Geol. Surv. Can. Bull. **588,** 193–209 (2007).

A. B. Ronov, A. A. Migdisov, and K. Khane, "Quantitative regularities in the composition evolution of silty–sandy rocks of the Russian Plate," Geochem. Int., No. 3, 312–336 (1995).

A. B. Ronov, and A. A. Migdisov "Quantitative regularities in structure and composition of sedimentary sequences of the East European Platform and Russian Plate and their setting among ancient platforms of the world," Lithol. Miner. Resour. **31** (5), 451–475 (1996).

B. P. Roser and R. J. Korsch, "Determination of tectonic setting of sandstone–mudstone suites using SiO_2 content and K_2O/Na_2O ratio," J. Geol. **94**, 635–650 (1986).

M. Yu. Rumyantsev, Extended Abstract of Candidate's Dissertation in Geology and Mineralogy (IGM SO RAN, Novosibirsk, 2001) [in Russian].

A. I. Rusin, "Late Vendian collision in the Ural zone: myth or reality? in *Yearbook-1997*, IGG UrO RAN, Yekaterinburg, 1998), pp. 56–61 [in Russian].

K. M. Ryan and D. M. Williams, "Testing the reliability of discrimination diagrams for determining the tectonic depositional environment of ancient sedimentary basins," Chem. Geol. **242**, 103–125 (2007).

M. A. Semikhatov, *Stratigraphy and Geochronology of the Proterozoic* (Nauka, Moscow, 1974) [in Russian].

A. Shalaby, K. Stuwe, H. Fritz, and F. Makroum, "The El Mayah molasse basin in the Eastern Desert of Egypt," J. Afr. Earth Sci. **45**, 1–15 (2006).

G. G. Shemin, *Geology and Petroleum Prospects of the Vendian and Lower Cambrian of the central Siberian Platform* (Nepa–Botuoba and Baikit anteclise, and Katanga Saddle) (SO RAN, Novisibirsk, 2007) [in Russian].

A. V. Sochava, L. V. Korenchuk, E. A. Pirrus, and S. B. Felitsyin, "Geochemistry of the Upper Vendian sediments of the Russian Platform," Litol. Polezn. Iskop., No. 2, 71–89 (1992).

T. M. Sokut, "Lithological and geochemical features of the Upper Vendian and Lower Cambrian Mudstones of the East European Platform," Dokl. DNTU. Geological-Mining Ser. **206,** 12–19 (2012).

V. P. Tverdokhlebov, "Piedmone fans and Aeolian sediments as indicator onf arid climate in the eastern European Russia at the beginning of Triassic," Izv. Vyssh. Uchebn. Zaved., Ser. Geol. Razvedka, No. **1**, 53–57 (2001).

S. P. Verma and J. S. Armstrong-Altrin, "New multidimensional diagrams for tectonic discrimination of siliciclastic sediments and their application to Precambrian basins," Chem. Geol. **355**, 117–133 (2013).

V. A. Vernikovsky, A. Yu. Kazansky, N. Yu. Matushkin, D. V. Metelkin, and Yu. K. Sovetov, "The geodynamic evolution of the folded framing and the western margin of the Siberian craton in the Neoproterozoic: geological, structural, sedimentological, geochronological, and paleomagnetic data," Russ. Geol. Geophys. **50** (4), 372–387 (2009).

R. G. Yazeva and V. V. Bochkarev, *Geology and Geodynamics of the South Urals* (UrO RAN, Yekaterinburg, 1998) [in Russian].

Translated by N. Kravets